

## Study on the thermal decomposition kinetics of nano-sized calcium carbonate\*

LI Dai-xi(李代禧)<sup>†1,2</sup>, SHI Hong-yun(史鸿运)<sup>†1</sup>, DENG Jie(邓洁)<sup>1</sup>, XU Yuan-zhi(徐元植)<sup>2</sup>

(<sup>1</sup> Chemistry Department, Guizhou University, Guizhou 550025, China)

(<sup>2</sup> Chemistry Department, Zhejiang University, Hangzhou 310027, China)

E-mail: <sup>†1</sup>hyshi@tmail.gzu.edu.cn; <sup>†2</sup>dxli75@sohu.com

Received Oct. 8, 2002; revision accepted Dec. 2, 2002

**Abstract:** This study of the thermal decomposition kinetics of various average diameter nano-particles of calcium carbonate by means of TG-DTA (thermogravimetry and differential thermal analysis) showed that the thermal decomposition kinetic mechanisms of the same crystal type of calcium carbonate samples do not vary with decreasing of their average diameters; their pseudo-active energy  $E_a$ ; and that the top-temperature of decomposition  $T_p$  decreases gently in the scope of micron-sized diameter, but decreases sharply when the average diameter decreases from micron region to nanometer region. The extraordinary properties of nano-particles were explored by comparing the varying regularity of the mechanisms and kinetic parameters of the solid-phase reactions as well as their structural characterization with the variation of average diameters of particles. These show that the aggregation, surface effect as well as internal aberrance and stress of the nano-particles are the main reason causing both  $E_a$  and  $T_p$  to decline sharply with the decrease of the average diameter of nano-particles.

**Key words:** Nano-particle, Aggregation, Non-isothermal kinetics, Surface effect, Phase interface reaction.

**Document code:** A

**CLC number:** O614.23; O643.12

## INTRODUCTION

There are few of quantitative thermal analysis (TA) investigations (Mulokozi, 1992) of the governing relations between the parameters of solid phase reaction kinetics and the average diameters of ultra fine calcium carbonate and the effects of fine particles on their solid phase reaction kinetics. And a few of them were only limited to particles with size of several microns (Ortega *et al.*, 1990). This paper reports the results of TA study on the correlation between the solid phase reaction kinetics mechanisms' parameters and the varying average diameters of nano-sized calcium carbonate.

## EXPERIMENTS AND METHODS

### 1. Samples and experiential conditions

The 40 nm to 1.25  $\mu\text{m}$  calcite and aragonite samples used in the study were synthesized by

using microtherm carbonization method and double-decomposition reaction method under various temperatures, respectively. The DT-40 thermal analyzer made in Japan Shimadzu was used. Amorphous  $\text{Al}_2\text{O}_3$  was used as a reference. A verified standard A. R. (analytical reagent) calcium carbonate (common calcite) with average diameter of 5  $\mu\text{m}$  as determined by SEM (Scanning electron microscope) was used. The experimental conditions were: atmosphere of static air, heat rate of 10 K/sec.

### 2. Data analysis

A commonly used standard method using the Coats-Redfern integral equation and Anderson-Freeman differential equation was used to analyze the original data and to verify the mechanisms (Elder, 1998). The logarithmic equations were as follows:

$$\ln g(\alpha) - \ln(T - T_0) = \ln \frac{A}{\beta} - \frac{E}{RT}$$

\* Project supported by Guizhou Province Natural Science Foundation of China

† Author for correspondence

and

$$\ln \left( \frac{d\alpha/dT}{f(\alpha) \left[ \frac{E(T-T_0)}{RT^2} + 1 \right]} \right) = \ln \frac{A}{\beta} - \frac{E}{RT}$$

Where  $g(\alpha)$  and  $f(\alpha)$  are integral and differential mechanism function, respectively.  $\beta$ ,  $A$ ,  $R$ , and  $E_a$  are heat rate, frequency factor, gas constant, and pseudo-active energy, respectively.

### 3. Kinetics experiments

Before the experiments, pure zinc and calcium oxalate were used to modulate temperature and baseline of the TA curve respectively. Then 5 mg sample of calcium carbonate was weighted and placed into the thermal analyzer, to conduct thermal analysis experiments.

## RESULTS

### 1. The decomposition mechanism and kinetics parameters of calcite samples

The verified sample's TG-DTA curves are shown in Fig. 1.

The results of the standard method proved that the phase interface reaction mechanisms with three-dimensional spherical shrink (R3) were the most ideal ones; so that the thermal decomposition of the verified sample should in accordance with the mechanism R3, and with the R3 mechanism function:  $f(\alpha) = (1 - \alpha)^{2/3}$ . These mechanism results were the same as those obtained by the method using the properties of

the TA curves (Dollimore, 1996). The verified sample's pseudo-active energy  $E_a$  was about 234.128 kJ/mol – 228.795 kJ/mol. And its mechanism and  $E_a$  values match very well with related references (Sharp *et al.*, 1969; Wang *et al.*, 1995).

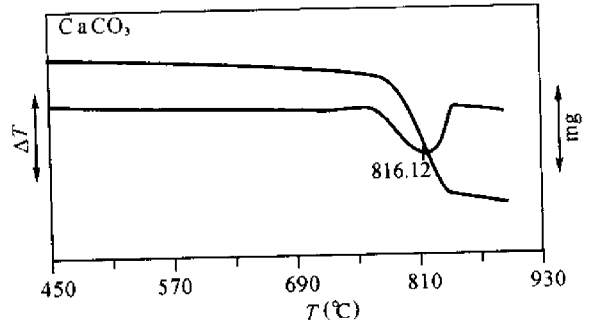


Fig.1 TG-DTA curves of the verified calcite

In order to study the effect of diameters on the solid-phase reaction kinetics, four calcite samples with TA curves were analyzed using the standard method combined with both Coats-Redfern's integral equation and Anderson-Freeman's differential equation. The final results (Table 1) indicated that all calcite samples decomposed thermally in according to the same mechanism and mechanism function of the verified calcite sample. The pseudo-active energy  $E_a$  and peak-temperature of thermal decomposition  $T_p$  decreased with the decrease of the average diameter of particles. The decrease of the pseudo-active energy  $E_a$  was very obvious.

Table 1 Kinetics parameters and mechanism of some calcite samples

| Samples(No) | $d$                | $T_p$ (K) | Mech. | $E_a$ (kJ/mol) | $A$ ( $\text{min}^{-1}$ ) | $R$        |
|-------------|--------------------|-----------|-------|----------------|---------------------------|------------|
| C01         | 5.0 $\mu\text{m}$  | 1089.5    | R3(f) | 234.128        | $4.3275 \times 10^{12}$   | -0.9984686 |
|             |                    |           | R3(g) | 228.795        | $1.9712 \times 10^{11}$   | -0.9982535 |
| C02         | 1.25 $\mu\text{m}$ | 1017.5    | R3(f) | 155.571        | $2.5034 \times 10^7$      | -0.9986186 |
|             |                    |           | R3(g) | 152.839        | $2.7748 \times 10^6$      | -0.9991508 |
| C03         | 800 nm             | 1003.9    | R3(f) | 146.230        | $1.2807 \times 10^8$      | -0.9993470 |
|             |                    |           | R3(g) | 141.750        | $4.8375 \times 10^5$      | -0.9965646 |
| C04         | 399 nm             | 988.1     | R3(f) | 139.043        | $7.5000 \times 10^7$      | -0.9998547 |
|             |                    |           | R3(g) | 133.786        | $2.6147 \times 10^5$      | -0.9976337 |
| C05         | 40 nm              | 955.5     | R3(f) | 102.948        | $1.4668 \times 10^5$      | -0.9984544 |
|             |                    |           | R3(g) | 98.8988        | $3.3025 \times 10^6$      | -0.999393  |

## 2. Decomposition mechanism and kinetics parameters of aragonite samples

The TA curves of aragonite samples were analyzed using the above-mentioned method. The results (Table 2) indicate that the mechanisms of

all the aragonite samples were the random nucleation mechanism (F1) according with the F1 mechanism function  $f(\alpha) = 1 - \alpha$ . The correlation of the calcite samples could be found in the same way.

**Table 2 Kinetics parameters and mechanism of some aragonite samples**

| Samples(No) | $d$                | $T_p$ (K) | Mech. | $E_a$ (kJ/mol) | $A$ ( $\text{min}^{-1}$ ) | $R$        |
|-------------|--------------------|-----------|-------|----------------|---------------------------|------------|
| A01         | 5.18 $\mu\text{m}$ | 984.3     | F1(f) | 143.823        | $3.6910 \times 10^8$      | -0.9876734 |
|             |                    |           | F1(g) | 137.026        | $1.2551 \times 10^6$      | -0.9977251 |
| A02         | 1.60 $\mu\text{m}$ | 973.2     | F1(f) | 137.010        | $2.6898 \times 10^7$      | -0.9988632 |
|             |                    |           | F1(g) | 136.203        | $3.7989 \times 10^6$      | -0.9899623 |
| A03         | 600 nm             | 967.6     | F1(f) | 136.969        | $9.9165 \times 10^7$      | -0.9887920 |
|             |                    |           | F1(g) | 136.152        | $1.3539 \times 10^6$      | -0.9978461 |
| A04         | 350 nm             | 963.4     | F1(f) | 116.564        | $4.5321 \times 10^6$      | -0.9989765 |
|             |                    |           | F1(g) | 112.398        | $5.6432 \times 10^7$      | -0.9998756 |
| A05         | 50 nm              | 943.5     | F1(f) | 100.838        | $3.5871 \times 10^7$      | -0.9821471 |
|             |                    |           | F1(g) | 96.734         | $2.1196 \times 10^7$      | -0.9981609 |

## DISCUSSIONS

### 1. The effect of diameter on decomposition temperature

The graph of logarithms of the decomposition temperature  $T_p$  versus average diameter (Fig. 2) shows that the  $T_p$  of all the ultra fine calcium carbonate decreases with the decrease of the average diameter of particles. Calcite's  $T_p$  decreased gently with the decrease of the average diameter of the micron-size particles; but decreased sharply when the average diameter decreased from micron-size to nanometer-size. The  $T_p$  of the 40nm calcite was 132K less than that of  $T_p$  of common verified calcite. The rate of  $T_p$  decrease of nano-sized calcite samples was greater than micrometer size samples. The  $T_p$  change of the aragonite samples was not as large as that of the calcite samples. But no matter whether the aragonite samples were nano-sized or micron-sized, all their  $T_p$  were lower than those of the calcite samples. The  $T_p$  of the aragonite samples had the same sharp decline when their diameters decreased from micron-size to nano-size, and the

$T_p$  of the nano-aragonite samples was about 145.8K lower than that of the common verified calcite. There are many explanations for the  $T_p$  decrease with decreasing diameters. Some scholars explained it was due to thermal resistance and cold-itself effect (Van Dooren *et al.*, 1982) as well as the number of the active spots (Liu, 1991). Their explanations were rational, but did not reach into the nature of the matter. So they could not explain it reasonably and fully. We consider that the alteration of the nano-crystalline material's internal microstructure is the real cause (Meyer, 1994).

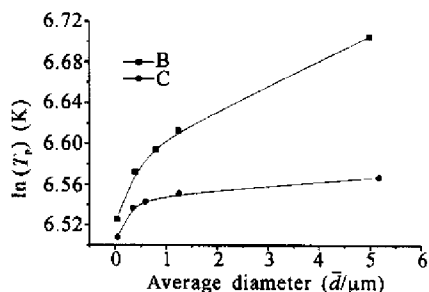


**Fig. 2 Curves of  $\ln(T_p)$  vs  $\bar{d}$**

(B: Curves of calcite; C: Curves of aragonite)



Fig.3 Electron diffraction of the nano-calcite

Firstly, the crystalline grade of the nano-calcite was so bad that we could see it from the electron diffraction (Fig. 3) indicating obvious aberration and stresses inside the crystalline structure of the nano-sized calcium carbonate samples, whose aberration and stresses may be considered as main causative reasons for the easy decomposition of the nano-calcium carbonate.

Secondly, the result of scanning electron microscopy (SEM) (Fig. 4) and transmission electron microscopy (TEM) (Fig. 5) showed that the crystalline perfection of the nano-calcite was gradually ruined and soft reunites arises in the nano-crystalline structure of calcite sample with various average diameters. Which implies that the particles aggregate together when their size decreased into the nano-meter region. And the calcium carbonate become nano-material and get into the medium scope state (Feng *et al.*, 2001). The aggregation effect causes the aberration and stresses in the crystalline structure of materials. On the other hand, the transformation of the regular surface of ultra-fine particles' into irregular spherical surface increases the surface/volume ratio. This indicates that the surface effect and stress produced inside the crystalline are

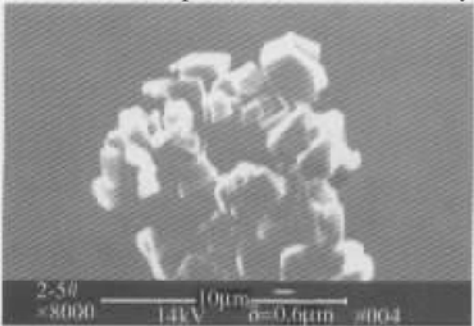


Fig.4 SEM of 1.25 $\mu$ m calcite

too large to neglect. Therefore, the aggregation effect and surface effect are two main reasons for the sharp decrease of the  $T_p$ .

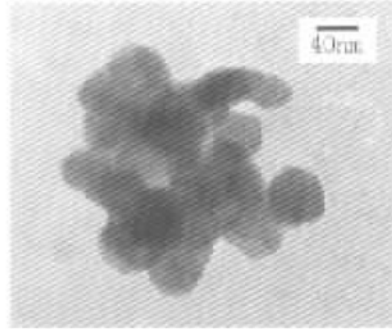


Fig.5 TEM of nano-calcite

## 2. The effect of diameter on active energy

The curve of the pseudo-active energy  $E_a$  versus average diameter  $\bar{d}$  in semi-logarithmic coordinates (Fig. 6) shows that the change of the pseudo-active energy  $E_a$  with the various diameters follows the same rule as that of peak-temperatures of thermal decomposition  $T_p$ . The only difference is that the pseudo-active energy  $E_a$  of nano-calcite sharply decreased by about 132 kJ/mol, and while that of nano-aragonite sharply decreased by only about 41 kJ/mol. This indicated the value of the pseudo-active energy  $E_a$  is related to the degree of the difficulty of the solid phase reaction.

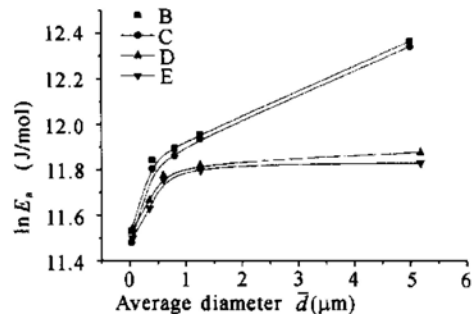


Fig.6 Curves of  $\ln E_a$  vs  $\bar{d}$

- B: Curves of calcite by differential equation;
- C: Curves of calcite by integral equation;
- D: Curves of aragonite by differential equation;
- E: Curves of aragonite by integral equation.

There are three causative reasons for the decrease of the pseudo-active energy  $E_a$ . Firstly,

the existence of the aberration and stress inside the crystalline structure of ultra-fine material is one of the dominant causative reasons for the pseudo-active energy  $E_a$  to decrease sharply. The existence of the aberration and stress makes the atoms inside crystalline rearrange to a new stabilization or equilibrium. Secondly, the aberration and stress inside the crystalline structure of ultra-fine material obviously reduces the crystal lattice energy, resulting in the sharp decrease of the pseudo-active energy  $E_a$ . Thirdly, the surface and aggregation effects increased sharply as a result of the decrease of average diameter, and finally led to easy decomposition of the sample material.

Molecular level investigation of the calcium carbonate surface revealed minimal reconstruction of the surface. The newly exposed surface was out of equilibrium. If there is scarcity of atoms, the dangling bonds are satisfied as much as possible by rearrangement of bonding configuration and surface structure. After cleavage, surface Ca atom share electrons with only five or fewer O atoms. This probably results in stronger CaO bonds at the surface. Finally, this not only can make it react most rapidly with the contacting medium but also can change the shape of the nanocrystalline structure (Mao *et al.*, 1997).

Additionally, the decrease of the average diameters of ultra-fine calcite makes the reactions of phase boundary movement transfer from long-range to short-range; and for ultra-fine aragonite, the reactions of random nucleation occur easily. This explains, from another point of view, why the pseudo-active energy  $E_a$  of the decomposition reaction decreases sharply when the average diameter becomes nano-size.

### 3. Comparison of the pseudo-active energies between calcite and aragonite

Fig. 6 shows that the  $E_a$  of calcite samples are larger than that of aragonite samples with the same average diameter. The difference of the  $E_a$  between calcite and aragonite follows the same correlation of  $T_p$  and  $E_a$  with the decrease of the average diameters (Fig. 7). This difference can be obtained from the data on the two curves in the Fig. 5 because the given points on the curve represent the  $E_a$  values of the various calcium carbonate samples, respectively. The formula is as follows:

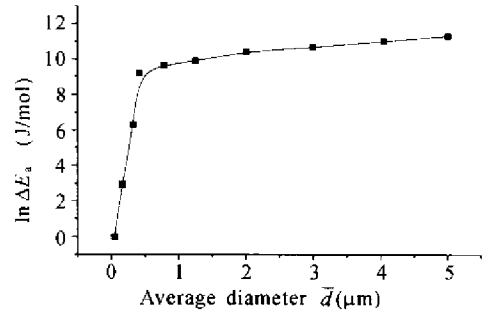


Fig. 7 Curve of  $\ln \Delta E_a$  vs  $d$

$$\Delta E_a = \frac{1}{2} [(E_f + E_g)_{\text{calcite}} - (E_f + E_g)_{\text{aragonite}}]$$

Fig. 7 indicates that the difference in the pseudo-active energies of calcite and aragonite decrease with the decrease of the average diameters. When the micron-particles transform into nano-particles, the difference of the active energies between calcite and aragonite would sharply decline and finally the value of the difference approaches to zero, namely,  $\Delta E_a \rightarrow 0$ .

Regarding the crystalline structure, calcite is octahedral. Namely, the coordination number of the  $\text{Ca}^{2+}$  cation is 6, while aragonite is orthorhombic, and the coordination number of its cation is 9. The extra ligands  $\text{CO}_3^{2-}$ , which take part in the coordination of the  $\text{Ca}^{2+}$  cation in the aragonite, weaken the ionic bond between the  $\text{CO}_3^{2-}$  anion and  $\text{Ca}^{2+}$  cation. According to the mechanism of reactive crystallization of  $\text{CaCO}_3$  polymorphs from  $\text{Ca}(\text{OH})_2$  suspensions, the aragonite crystallizes earlier than calcite under some conditions (Mitsutaka *et al.*, 2002). It was reported that aragonite is more active than calcite, and can even transform into calcite during the time of decomposition. But the solid-phase transformation is slow and not completed in atmosphere of dry air. Therefore, aragonite decomposed easier than calcite, and the pseudo-active energy of aragonite also is smaller than that of calcite.

The existence of many defects in crystalline material can facilitate the nucleation and diffusion resulting from decomposition reaction (Bezjak *et al.*, 1993). When the size of the particles reduces into nano scale, the number of the crystal defects would increase so rapidly that it causes the whole crystal crumble. Therefore, the

decrease of the diameter is very beneficial for the decomposition of calcite. However, for micron-sized aragonite, the decrease of the diameter only benefits the nucleation of decomposition. The change of the pseudo-active energy  $E_a$  of calcite is larger than that of aragonite. When the crystal structures of both types of calcium carbonate are on the verge of collapse, their pseudo-active energies will be approach to equal.

The difference of two pseudo-active energies of calcite and aragonite becomes small with the decrease of their diameters. It can well be imagined that the diffusion will be easier when the diameter of nano-particle decreases to some extent. Accordingly, the crystalline structure of calcite will be almost the same as that of aragonite, and it will be difficult to distinguish them from each other. In this case, both types of calcium carbonate will decompose according to mechanism F1, and their pseudo-active energies will be consistent close to each other.

### 3. The effect of diameter on frequency factor $A$

The so-called frequency factor represents the actual collision frequency of micro-particles in a unit of volume in nature. In this paper, the frequency factor  $A$  of calcite decreases with the decrease of particle diameter but the frequency factor  $A$  of aragonite does not, and the change is small. It is paradoxical that the reactivity is consistent with the actual collision frequency. But if we deeply probe into the problem, we can find that it is the serious crystalline imperfection in the nano-calcite that caused the frequency factor  $A$  of calcite to decrease. Although the aragonite nano structure is very relaxed and loose, the effect of the particle diameter on it is small.

## CONCLUSIONS

From the above discussion, it can be concluded that the thermal decomposition kinetic mechanisms of calcium carbonate do not vary with decreasing of their average diameters. The reactivity of the micro-particles is sharply en-

hanced when the average diameter decreases from the micron region to nanometer region. The aggregation and surface effect as well as internal aberration and stresses of the nano-particles are considered as the main causes of the enhanced reactivity of the micro-particles.

## References

- Bezjak, A., Tkalec, E., Ivankovic, H. and Ereš, M., 1993. Determination of kinetic parameters for nucleation and growth from DTA data. *Thermochim Acta*, **221**: 23 – 39.
- Dollimore, D., 1996. The kinetic interpretation of the decomposition of calcium carbonate by uses of relationships other than the Arrhenius equation. *Thermochim Acta*, **13**: 282 – 283;
- Elder, J. P., 1998. The “ $E-\ln(A)-f(\alpha)$ ” triplet in non-isothermal reaction kinetics analysis. *Thermochimica Acta*, **318**: 229 – 238.
- Feng, C.J. and Xu, Y.Z., 2001. State of arts on chemistry of ordered molecular aggregate. *Progress in Chemistry*, **13**(5): 329 – 336(in Chinese with English abstract).
- Liu Z.H., 1991. Thermal Analysis Introduction. Chemistry-Industry Press, Beijing, p.73(in Chinese with English abstract).
- Mao, Y. and Siders, P. D., 1997. Molecular Hartree-Fock model of calcium carbonate. *Journal of Molecule Structure (Theochem)*, **419**: 173 – 184.
- Meyer, K., 1994. Thermal analysis and microstructure of solids and solid state reactions. *Thermochim Acta*, **349** (1 – 3): 84 – 90.
- Mitsutaka, K., Haruo, K., Atsunari, Y. and Hirokatsu, M., 2002. Controlling factors and mechanism of reactive crystallization of calcium carbonate polymorphs from calcium hydroxide suspensions. *Journal of Crystal Growth*, **236**: 323 – 332.
- Mulokozi, A. M., 1992. The thermal decomposition kinetics of cadmium carbonate powder. *Thermochimica Acta*, **202**: 17 – 23.
- Ortega, A., Akhouayri, S., Rouquerol, F. and Rouquerol, J., 1990. On the suitability of controlled transformation rate thermal analysis (CRTA) for kinetic studies: 1. Determination of the activation energy by rate-jump method. *Thermochim Acta*, **163**: 25.
- Sharp, J. H. and Wentworth, S. A., 1969. Kinetic analysis of thermogravimetric data. *Analytical Chemistry*, **41** (14): 2060 – 2062.
- Van. Dooren, A. A. and Müller, B. W., 1982. Effects of heating rates and particle sizes on DSC peaks. *Thermochimica Acta*, **54**: 115 – 129.
- Wang, Y. and Thomsom, W. J., 1995. The effect of sample preparation on the thermal decomposition of  $\text{CaCO}_3$ . *Thermo him Acta*, **255**: 383 – 390.